Int. J. Solids Structures, 1973, Vol. 9, pp. 843 to 861. Pergamon Press. Printed in Great Britain

THE DYNAMIC FIELD OF A GROWING PLANE ELLIPTICAL SHEAR CRACK†

PAUL G. RICHARDS

Lamont–Doherty Geological Observatory of Columbia University, Palisades, New York 10964

Abstract—The radiation for a three-dimensional problem of brittle fracture is investigated. A crack is presumed to nucleate at a point in an infinite pre-stressed elastic medium, and the crack subsequently grows steadily with subsonic rupture velocities, maintaining the shape of an ellipse. Shear stresses are relieved by the crack, and exact solutions are derived for the acceleration and stress-rate (at every point of the medium) in terms of single integrals and algebraic expressions. The solutions are evaluated analytically at wavefronts and singularities, and numerically, at different points in the medium, for different growth rates of the crack.

1. INTRODUCTION

DESPITE the simplifying assumptions of modeling motion in solid media by the methods of linear elasticity, the catalogue of known solutions to dynamic crack problems is still small. Reasons for this lie both in the inherent difficulty of mixed boundary value problems (for which linear combinations of a field variable and its derivatives are known only on restricted regions of a two-dimensional surface), and in the necessity of dealing with two types of motion (irrotational and solenoidal), which are coupled by a stress-free surface. These known solutions have, however, played an important role in our understanding of a wide variety of material processes.

The early investigations concerned two-dimensional tensile problems, of cracks moving in a medium under uniform tension normal to the crack. Thus, Yoffe [1] examined the case of a straight tensile crack, of constant length, and moving with constant velocity. She showed that if the crack velocity exceeds a critical value (which is about 0·6 times the shear wave velocity) then the maximum tensile stress (in the vicinity of the crack tip) is no longer normal to the direction of crack propagation. She suggested this as the explanation of why observed cracks, in fractured glass and cellophane, have a tendency to curve. Broberg [2] solved the problem of a bilateral tensile crack, and was one of the first to show that if the crack-tip velocity, in brittle fracture, is constant, it should be the (Rayleigh) surface-wave velocity. Baker [3] obtained solutions for the case in which a semi-infinite tensile crack suddenly appears, and grows with constant velocity. He calculated the time variation of the tensile stress at a fixed point on the line of fracture, as the tip of the crack approaches. More recently, Kostrov [4] and Craggs [5] have obtained solutions for the three-dimensional tensile problem of a growing circular crack.

The radiation from propagating shear cracks is less well known than that from tensile cracks. Understanding properties of such radiation is, however, of considerable importance in studying earthquake faulting, since we may thereby hope to infer mechanical and geometrical parameters of the region of rupture, and so improve our comprehension of the earthquake mechanism. (See Kostrov [6] for a review.) Published solutions, for dynamic

† Contribution No. 1957.

crack propagation in media subjected to homogeneous shear, include the work of Kostrov [7], who investigated two-dimensional bilateral cracks, and also the three-dimensional case of a growing circular crack. Kostrov [8] considered criteria of failure, and showed how to calculate the velocity of brittle rupture for a longitudinal shear crack (in which displacement is everywhere parallel to the line of rupture). Burridge [9] gave a numerical treatment of bilateral cracks which stop growing after a certain time, and Burridge and Willis [10] obtained a solution for radiation from a growing elliptical crack in an anisotropic solid.

Apart from the displays in [9], these authors have not computed the radiation implied by their solution formulae. Indeed, in the three-dimensional problems of most interest, their solutions are usually given as double integrals which are not readily amenable to computation. In this paper, I show that the problem of an elliptical shear crack, growing in a prestressed medium, can be cast into a form soluble by the Cagniard–de Hoop methods developed by Gakenheimer and Miklowitz [11] and Gakenheimer [12] for moving sources. This problem is a generalization of the circular geometry examined in [7], and a specialization (to shear fracture in an isotropic medium) of the discussion in [10]. Fortunately, however, the solution given here is easily evaluated, and several features of the radiated fields are displayed below.

2. MATHEMATICAL FORMULATION

An infinite homogeneous elastic medium is initially in a state of uniform stress, denoted by the tensor $\boldsymbol{\sigma}^0$. After time $t = 0$, an elliptical plane shear crack starts to grow in the medium. With an appropriate choice of Cartesian coordinates, the crack surface is defined (see Fig. 1) by

$$S(t) = \{z = 0 : x^2/\sigma^2 + y^2/v^2 \leq t^2\} \qquad (0 < \sigma < c_s, 0 < v < c_s),$$

a formula which incorporates the assumptions that crack growth (i) is steady (σ and v are constants), and (ii) has rupture velocities along each axis which are less than the shear speed c_s. The shear tractions are "relieved" on the crack surface—that is, the yz and zx components of stress on $S(t)$ are dropped to new values which (iii) are assumed to be constant over the crack surface, equal to σ^1_{yz} and σ^1_{zx} (say). These constants would be zero if the crack surface could sustain no shearing traction. A more practical example of their value is suggested by linking the concept of dynamic friction on the crack surface with a

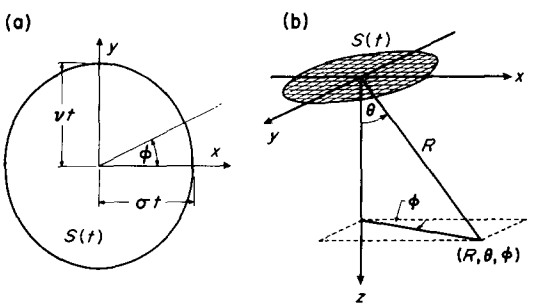

FIG. 1. Parameters for a growing elliptical crack: (a) the plane $z = 0$, seen from the side with $z > 0$; (b) the definition of spherical polar coordinates (R, θ, ϕ). Azimuth angle ϕ is taken between the plane $y = 0$, and the plane containing the field point and the z-axis.

result pointed out by Burridge [9], that the zz stress component throughout the plane of the crack remains constant at all times. One could then take

$$\sigma^1_{yz} = \sigma^0_{zz}\mu_f \sin\psi,\ \sigma^1_{zx} = \sigma^0_{zz}\mu_f \cos\psi, \tag{1}$$

in which ψ specifies the frictional force direction, and μ_f is the coefficient of dynamic friction. The assumption that shear stresses are constant over the (moving) crack surface is not physically unreasonable in seismic problems, since the crack is spreading over a plane (a geological fault) of pre-existing weakness. It is a less reasonable assumption for genuine fracture in virgin materials, since then the surface energy of creating new crack surface is significant, and can control the characteristics of the rupture. Whatever the values assumed for shearing stresses on the crack surface, the problem remains (in the case of subsonic rupture velocities) that we do not know from what immediate value the stress is dropped. For, although the initial shears σ^0_{yz} and σ^0_{zx} are known, a point P in the plane $z = 0$ is in general influenced after $t = 0$ (but before the crack arrival) by prior radiation from the crack. It is this fact which leads in general to a mixed boundary value problem, but results of [9] and [10] permit a relatively straightforward boundary value problem to be set up, for the present crack geometry. To describe these results we let $\mathbf{u}$ be displacement away from the initial (static, prestressed) position, with $\boldsymbol{\tau}$ as the derived stress tensor (so that $\boldsymbol{\sigma}^0 + \boldsymbol{\tau}$ is the total stress). The remark preceding equation (1) implies that

$$\tau_{zz} = 0 \quad \text{on } z = 0. \tag{2}$$

By guessing the form of displacement discontinuity across the crack (and subsequently verifying that all the necessary properties of this brittle fracture problem are reproduced), it is shown in [10] that the relative displacement of opposite crack faces takes the form

$$[u_x, u_y]^{z=0^+}_{z=0^-} = 2(a, b)(t^2 - x^2/\sigma^2 - y^2/v^2)^{\frac{1}{2}} \quad \text{on } S(t), \tag{3}$$

in which a and b are two constant velocities, proportional to the stress drops $\sigma^0_{zx} - \sigma^1_{zx}$, $\sigma^0_{yz} - \sigma^1_{yz}$ respectively. To solve the radiation in, say, the half space $z \geq 0$, we may use the result (see [9]) that u_x, u_y are odd functions of z, and obtain from (3) two further boundary conditions

$$(u_x, u_y) = \begin{cases} (0, 0) & \text{on } z = 0^+ \text{ but off } S(t) \\ (a, b)(t^2 - x^2/\sigma^2 - y^2/v^2)^{\frac{1}{2}} & \text{on } z = 0^+ \text{ and } S(t). \end{cases} \tag{4}$$

Note that the displacement of the origin has (x, y) components (at, bt) after rupturing, so the (a, b) velocities are just velocity components for the center of the crack.

Solution in the half space $z \geq 0$

Introducing Lamé potentials Φ and $\mathbf{A}$ which generate $\mathbf{u}$ via $\mathbf{u} = \nabla\Phi + \nabla \times \mathbf{A}$, we have

$$c_d^2 \nabla^2 \Phi = \partial^2\Phi/\partial t^2, \qquad c_s^2 \nabla^2 \mathbf{A} = \partial^2 \mathbf{A}/\partial t^2 \tag{5}$$

and

$$\nabla \cdot \mathbf{A} = 0 \tag{6}$$

where c_d is the dilatational wave speed. Initial conditions are that Φ, $\partial\Phi/\partial t$, $\mathbf{A}$, $\partial\mathbf{A}/\partial t$ are zero at time $t = 0$.

Taking a one-sided Laplace transform of time ($^-$), and bilateral Fourier transforms of x and y ($^{\approx}$), the boundary conditions (2) and (4) become

$$\tilde{\bar{\tau}}_{zz}(k, v, z, s) = 0, \qquad (\tilde{\bar{u}}_x, \tilde{\bar{u}}_y) = (a, b)\frac{4\pi\sigma v}{(s^2 + k^2\sigma^2 + v^2 v^2)^2} \quad \text{on } z = 0^+ \tag{7}$$

where (k, v, s) are the transform variables corresponding to (x, y, t). It is then a simple manipulation to obtain transformed potentials satisfying (5)–(7), together with the initial conditions and radiation condition $|\mathbf{u}| \to 0$ as $z \to \infty$. Allowing $f(\mathbf{x}, t)$ to represent any one of the scalar dependent variables Φ, A_j, u_j, τ_{jk} ($j, k = x, y$ or z), the Laplace transform $\bar{f}$ can be obtained after two Fourier inversions as the sum of dilatational and shear contributions, $\bar{f}(\mathbf{x}, s) = \bar{f}_d(\mathbf{x}, s) + \bar{f}_s(\mathbf{x}, s)$, where

$$\bar{f}_\alpha(\mathbf{x}, s) = \frac{\sigma v c_s^2}{\pi s^2} \int_{-\infty}^{\infty} dk \int_{-\infty}^{\infty} dv \frac{F_\alpha(k, v, s)\, e^{i(kx+vy)-n_\alpha z}}{(s^2+k^2\sigma^2+v^2v^2)^2} \tag{8}$$

for $\alpha = d$ or s, in which F_α is given for 10 different dependent variables f by Table 1, and $n_\alpha = (k^2+v^2+s^2/c_\alpha^2)^{\frac{1}{2}}$. Since (8) is a solution in $z \geq 0$, we require $n_\alpha \geq 0$.

TABLE 1. A LIST OF THE INTEGRANDS APPROPRIATE IN EQUATION (8) FOR DIFFERENT DEPENDENT VARIABLES f. IN THE CASES OF u_x, u_y, τ_{zz}, RELATIONS BETWEEN F_d AND F_s ARE SHOWN WHICH ARE EQUIVALENT TO THE BOUNDARY CONDITIONS (7). μ IS THE RIGIDITY.

f	F_d	F_s
Φ	$2i(ak+bv)$	0
A_x	0	$-[akv+b(v^2+n_s^2)]/n_s$
A_y	0	$[a(k^2+n_s^2)+bkv]/n_s$
A_z	0	$i(av-bk)$
u_x	$-2k(ak+bv)$	$a(2k^2+s^2/c_s^2)+2bkv = -F_d+as^2/c_s^2$
u_y	$-2v(ak+bv)$	$2akv+b(2v^2+s^2/c_s^2) = -F_d+bs^2/c_s^2$
u_z	$-2in_d(ak+bv)$	$i(ak+bv)(k^2+v^2+n_s^2)/n_s$
τ_{zx}/μ	$4kn_d(ak+bv)$	$-(ak+bv)(4n_s-s^2/c_s^2n_s)k-an_ss^2/c_s^2$
τ_{yz}/μ	$4vn_d(ak+bv)$	$-(ak+bv)(4n_s-s^2/c_s^2n_s)v-bn_ss^2/c_s^2$
τ_{zz}/μ	$2i(k^2+v^2+n_s^2)(ak+bv)$	$-2i(ak+bv)(k^2+v^2+n_s^2) = -F_d$

The method of inversion, from $\bar{f}(s)$ to $f(t)$, may adequately be illustrated by examining further the case in which only the zx component of stress is relieved. That is, $\sigma_{yz}^0 = \sigma_{yz}^1$, and the constant b of (4) is zero. Note, however, that τ_{yz} may still be non-zero, on $z = 0$ but off $S(t)$.

We can expect the solution for the radiated field to contain just two wavefronts, concentric spheres of radii $c_d t$ and $c_s t$ at time t, and centered on the point of nucleation. Since the rupture velocities are subsonic, the crack surface remains within both wavefronts.

3. INVERSION METHOD, FOR A ZX-COMPONENT OF STRESS DROP

To demonstrate the inversion procedure for $\bar{f}$, it suffices to work with the scalar potential, the Laplace transform of which is

$$\bar{\Phi}(\mathbf{x}, s) = \frac{2a\sigma v c_s^2}{\pi s^2} \int_{-\infty}^{\infty} dk \int_{-\infty}^{\infty} dv \frac{ik\, e^{i(kx+vy)-n_d z}}{(s^2+k^2\sigma^2+v^2v^2)^2}.$$

Following the method of Gakenheimer and Miklowitz [11], we make the de Hoop transformation

$$k = (s/c_d)[q\cos\phi - w\sin\phi], \qquad v = (s/c_d)[q\sin\phi + w\cos\phi]$$

where $\phi = \tan^{-1}(y/x)$. After separating the resulting integrand into components even and odd in w, we find

$$\bar{\Phi}(\mathbf{x}, s) = \frac{C}{2s^3}\int_0^\infty dw \int_{-\infty}^{\infty} dq\, J(q, w, \phi)\, e^{-(s/c_d)(-iqr + m_d z)} \tag{9}$$

in which $C = 8a\Sigma N c_s^2/(\pi c_d)$, where $\Sigma = \sigma/c_d$ and $N = v/c_d$ are the normalized rupture velocities,

$$J = \frac{(E^2 + O^2)iq\cos\phi + 2EO(iw\sin\phi)}{(E^2 - O^2)^2}, \quad \text{where}$$

$$E = 1 + q^2 D + w^2 F, \qquad O = -2qw(\Sigma^2 - N^2)\cos\phi\sin\phi$$

with $D = \Sigma^2\cos^2\phi + N^2\sin^2\phi$, $F = \Sigma^2\sin^2\phi + N^2\cos^2\phi$ (so E and O are respectively even and odd, in either q or w) and $r = (x^2 + y^2)^{\frac{1}{2}}$, $m_d = (q^2 + w^2 + 1)^{\frac{1}{2}}$. We add the constraint $\mathrm{Re}\, m_d \geq 0$, which generalizes the previous $n_d \geq 0$, to permit interpretations with possibly complex values of q and w.

The real and imaginary parts of the integrand in (9) are respectively even and odd in q, yielding

$$\bar{\Phi}(\mathbf{x}, s) = \frac{C}{s^3}\,\mathrm{Re}\left\{\int_0^\infty dw \int_0^\infty dq\, J\, e^{-(s/c_d)(-iqr + m_d z)}\right\}. \tag{10}$$

To evaluate this result, we first consider path deformations in the first quadrant of the complex q-plane, for real and positive values of w (see Fig. 2). Relevant singularities of the integrand in (10) are then

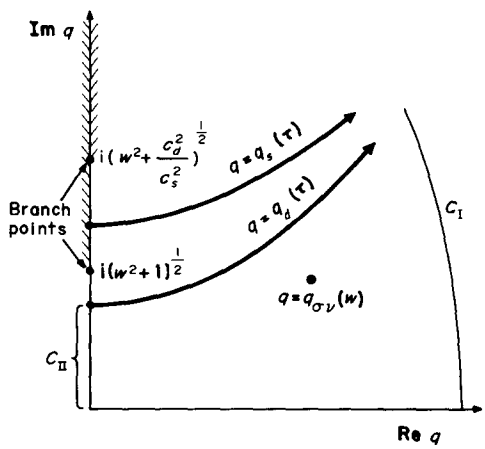

FIG. 2. Branch cuts, Cagniard paths, and the propagation pole $q_{\sigma v}$ in the first quadrant of the complex q-plane. Note that the Cagniard paths never intersect the branch cuts, since the branch point at $q = i(w^2 + 1)^{\frac{1}{2}}$ is present only for dilatational waves, which are inverted via $q = q_d(\tau)$. Hence, there are no head waves in the present problem.

(a) a branch point at $q = i(w^2+1)^{\frac{1}{2}}$, with a cut running up the imaginary q-axis, and
(b) a second order pole at $q = q_{\sigma v} \equiv [w\Delta + i(w^2\Sigma^2 N^2 + D)^{\frac{1}{2}}]/D$, where

$$\Delta = (\Sigma^2 - N^2)\cos\phi \sin\phi.$$

(The integrand has three other such poles, obtainable from $q_{\sigma v}$ by reflection in the two coordinate axes, and in the origin.)

The standard inversion procedure for (10) is to turn the q-integral into the Laplace transform (over time) of the w-integral. This implies a change in the order of integration, but first we make the identification of time as $t = (-iqr + m_d z)/c_d$, solving for q to obtain the first quadrant path

$$q = q_d(w, t) \equiv (\tau^2 - \tau_{wd}^2)^{\frac{1}{2}} \cos\theta + i\tau \sin\theta, \tag{11}$$

for $\tau \equiv c_d t/R \geq \tau_{wd} \equiv i(w^2+1)^{\frac{1}{2}}$, where (R, θ, ϕ) are the spherical polar coordinates shown in Fig. 1.

In deforming the q-integration in (10) from the real q-axis to the Cagniard (real time) path $q = q_d$, the residue from the pole at $q = q_{\sigma v}$ will be picked up if and only if w is such that q_d lies above $q_{\sigma v}$. It may be shown that the range of w for which this occurs is given by

$$w^2 G > D\cos^2\theta(1 - D\sin^2\theta), \quad \text{where} \quad G \equiv D\sin^2\theta(F + D\cos^2\theta) - \Sigma^2 N^2. \tag{12}$$

Thus, since $1 - D\sin^2\theta > 0$, the polar residue is to be included if and only if both
(i) $G > 0$ (which defines a region of the half-space $z \geq 0$), and
(ii) $w > w_{0d} \equiv [D\cos^2\theta(1 - D\sin^2\theta)/G]^{\frac{1}{2}}$.

Further points to note in deforming to the Cagniard path (see Fig. 2) are that the contribution from large arc C_I is vanishingly small, and from C_{II} is zero (since the integrand is pure imaginary). So, separating out the residue contribution to $\bar{\Phi}$, we have $\bar{\Phi}(\mathbf{x}, s) = \bar{\Phi}^{(1)} + \bar{\Phi}^{(2)}$ where

$$\bar{\Phi}^{(1)}(\mathbf{x}, s) = \frac{C}{s^3}\,\mathrm{Re}\left\{\int_0^\infty dw \int_{t_{wd}}^\infty J(q_d, w, \phi)\, e^{-st} \frac{c_d}{R}\frac{\partial q_d}{\partial \tau}\, dt\right\} \quad \text{and}$$

$$\bar{\Phi}^{(2)}(\mathbf{x}, s) = H(G)\frac{C}{s^3}\,\mathrm{Re}\left\{\int_{w_{0d}}^\infty 2\pi i\left[\left(\frac{\partial I}{\partial q} + \frac{isrI}{c_d} - \frac{sqzI}{c_d m_d}\right) e^{-(s/c_d)(-iqr + m_d z)}\right]_{q = q_{\sigma v}(w)} dw\right\} \tag{13}$$

where $H(x)$ is the Heaviside unit step function,

$$I(q, w, \phi) \equiv (q - q_{\sigma v})^2 J, \quad \text{and} \quad t_{wd} = \tau_{wd} R/c_d.$$

Inversion of $\bar{\Phi}^{(1)}$ to the time domain is thus obtained by interchanging the order of w- and t-integration, giving

$$\frac{\partial^3}{\partial t^3}\Phi^{(1)}(\mathbf{x}, t) = C\frac{c_d}{R}H(\tau - 1)\int_0^{T_d} \mathrm{Re}\left\{J(q_d(w, \tau), w, \phi)\frac{\partial q_d}{\partial \tau}\right\} dw, \tag{14}$$

where $T_d = (\tau^2 - 1)^{\frac{1}{2}}$.

We note the expected result, for three-dimensional Cagniard–de Hoop problems, that the solution is expressed in terms of a single integral. It is also seen that the solution is naturally expressed in terms of the third time derivative. This essentially is because the

third derivative is the first one discontinuous across the time $t = c_d/R$ (i.e. $\tau = 1$), the time of arrival of the P-wave from the initial point of nucleation of the crack. Corresponding results for displacement and stress are that the method of this paper leads naturally to formulae (like (14)) for acceleration $\ddot{u}$ and stress rate $\dot{\tau}$.

Inversion of $\bar{\Phi}^{(2)}$ to the time domain is accomplished by the method due to Gakenheimer and Miklowitz [11], who showed that the w-integral of residues in (13) could itself be converted to a Laplace transform integral, by finding an appropriate Cagniard path in the complex w-plane (see Fig. 3). The identification of time is clearly

$$t = (1/c_d)[-iqr + m_d z]|_{q = q_{\sigma v}(w)} \tag{15a}$$

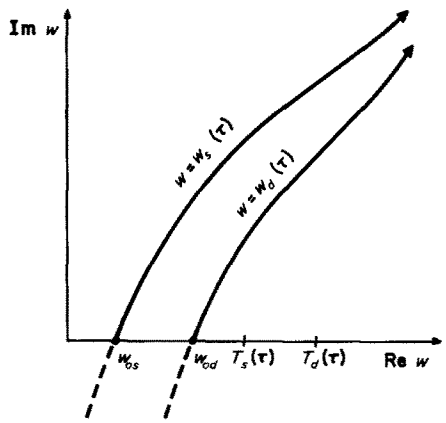

FIG. 3. Cagniard paths in the first quadrant of the complex w-plane.

and it is not difficult to show that (in the case $G > 0$) equation (15a) does define a path $w = w_d(t)$ in the first quadrant of the w-plane; that is, a path parameterized by real values of time t. The solution of (15a), for w as a function of t, unfortunately involves solution of a quartic, and the Cagniard path cannot be described in the simple analytic fashion of (11). However, there is no difficulty in numerically obtaining both the path and the derivative $(\partial w_d/\partial t)$. The method is described briefly below, the main features of the solution being a path which crosses into the first quadrant (from the fourth) at the point $w = w_{0d}$ at time

$$t = t_{0d} \equiv (w_{0d}^2 \Sigma^2 N^2 + D)^{\frac{1}{2}} R^2/(c_d r D) \tag{15b}$$

and which subsequently tends to the asymptotic value

$$w_d(t) \sim (c_d D t/R)/\{[D^2 + (\Delta + i\Sigma N)^2]^{\frac{1}{2}} \cos\theta - i(\Delta + i\Sigma N)\sin\theta\} \qquad \text{as } t \to \infty. \tag{15c}$$

The time domain inversion of (13) now follows immediately in the form

$$\frac{\partial^3}{\partial t^3}\Phi^{(2)} = 2\pi C H(G) H(t - t_{0d}) \operatorname{Re} i\left\{K\frac{\partial w_d}{\partial t} + \frac{\partial}{\partial t}\left\{L\frac{\partial w_d}{\partial t}\right\}\right\} \tag{16}$$

where $K = \partial I/\partial q$ and $L = (ir - qz/m_d)I/c_d$, and both K and L are obtained as functions of time from $I = I(q_{\sigma v}(w_d(t)), w_d(t), \phi)$.

Equation (16) concludes this description of the basic inversion procedure. To obtain the P-wave component of motion for other dependent variables (such as acceleration, or stress rate), one simply carries out the integration (14) with a different definition of J, and adds the result to the algebraic term (16) with corresponding definitions of K and L. To obtain the S-wave component of motion, the de Hoop transformation is again applied to $\bar{f}_s$ in equation (8), leading to the same second order pole $q_{\sigma v}(w)$ in the q-plane (Fig. 2), but to a new Cagniard path

$$q = q_s \equiv (\tau^2 - \tau_{ws}^2)^{\frac{1}{2}} \cos\theta + i\tau \sin\theta \tag{17}$$

for

$$\tau \equiv c_d t/R \geq \tau_{ws} \equiv i(w^2 + c_d^2/c_s^2)^{\frac{1}{2}}.$$

The S-wave term can then also be inverted to the time domain, using methods similar in all but minor detail to those already displayed for the P-wave potential. Since the analysis requires considerable algebraic manipulation, the complete solutions for acceleration and three components of the stress rate are given in the Appendix.

4. WAVEFRONTS AND SINGULARITIES

The system of wavefronts set up by a moving source (such as the present example of rupture) may easily be constructed by Huygen's Principle. The conical type of wavefront, spreading back from the moving source itself, is absent from the present analysis, because the crack tip moves subsonically. The only wavefronts generated are simply those spherical wavefronts (spreading with speeds c_d and c_s) which emanate from the origin of rupture itself, and which carry discontinuities in the dilatational and shear wave fields. It is a simple matter to quantify these discontinuities by evaluating formulae such as (14) and (A2) for times near the arrival times $\tau = 1$ and $\tau = c_d/c_s$ (i.e. $t = R/c_d$, $t = R/c_s$) for the two wave types, finding the discontinuities

$$\ddot{\mathbf{u}}_d(\mathbf{x}, t) = \frac{4\sigma v c_s^2 \cos\theta \sin\theta}{c_d^3(1 - D\sin^2\theta)^2}(a\cos\phi + b\sin\phi)\hat{\mathbf{x}}\frac{H(\tau - 1)}{R} \tag{18}$$

as $\tau \to 1$, where $\hat{\mathbf{x}}$ denotes a unit vector in the $\mathbf{x}$-direction, $D = (\sigma^2\cos^2\phi + v^2\sin^2\phi)/c_d^2$, and (R, θ, ϕ) are the spherical polar coordinates shown in Fig. 1;

$$\ddot{\mathbf{u}}_s(\mathbf{x}, t) = \frac{2\sigma v}{c_s(1 - D\tau_s^2\sin^2\theta)^2}\{\cos\theta[a, b, 0] - \sin\theta(a\cos\phi + b\sin\phi)$$
$$. [\sin 2\theta\cos\phi, \sin 2\theta\sin\phi, \cos 2\theta]\}\frac{H(\tau - \tau_s)}{R} \tag{19}$$

as $\tau \to \tau_s$, where $\tau_s = c_d/c_s$.

Formulae (18) and (19) are essentially approximations for the early motions of dilatational and shear waves in the radiated wave system. They are in agreement with results of Burridge and Willis [10] (after correction of a misprint in their equation (5.27)), and, as these authors have pointed out, the first motions are just those for a double couple modified by the factors $(1 - D\sin^2\theta)^{-2}$ for dilatation and $(1 - D\tau_s^2\sin^2\theta)^{-2}$ for shear waves.

A pseudo-wavefront

A feature of the solution forms (16) and (A3) is the discontinuity of the time-domain contributions from the residue terms. That is, for field points in the half-space $z \geq 0$ such that $G > 0$ (with G given by (12)), the algebraic terms giving the residue contribution have step-like discontinuities at "arrival" times $t = R\tau_{o\alpha}/c_d$ ($\alpha = d, s$). A similar phenomenon was noted by Gakenheimer and Miklowitz [11], in their solution for Lamb's problem with a moving source. Since these authors were able to show that such discontinuities appeared to be cancelled (in the case of a subsonic source) by matching discontinuities associated with the integral terms of (14) and the I_α of (A2), a similar property is to be expected in the present problem. This property is in fact found, and turns out to be the key to avoiding a numerically troublesome feature of the integrands in (14) and (A2). Namely, that at times near $t = R\tau_{0\alpha}/c_d$, these integrands have a second order pole which is sufficiently near the (real) path of integration ($0 \leq w \leq T_\alpha$) to require a large number of steps in any accurate integration scheme. The precise location of this pole in the complex w-plane is (from the definitions of E, O, and the Cagniard path in the complex q-plane), for dilatational waves, a solution to

$$w = [q\Delta - i(q^2\Sigma^2N^2 + F)^{\frac{1}{2}}]/F$$

where

$$q = q_d = (\tau^2 - w^2 - 1)^{\frac{1}{2}} \cos\theta + i\tau \sin\theta. \tag{20}$$

It may be shown that the solution for this w (as a function of time) is precisely the path $w = w_d(\tau)$ which is generated via (15). Two different roles are thus played by the Cagniard path in the w-plane: (a) it permits an algebraic expression to be obtained for part of the total solution in the time domain; and (b) the remaining part of the solution, a single integral, is complicated by a numerically troublesome singularity which, as time increases, also follows the Cagniard path. For a receiver in the region $G > 0$, this singularity actually crosses the path of numerical integration at just the time ($t = R\tau_{0d}/c_d$, for dilatational terms) at which the algebraic term starts to contribute.

Several examples of the path $w = w_d(\tau)$ are shown in Fig. 4, for a particular choice of velocities c_s, σ, ν, and of azimuth ϕ. The examples are for different values of the angle θ, and in all cases $G > 0$, so that the paths do cross the real w-axis from the fourth quadrant to the first. It may be shown that $0 \leq w_{0d} \leq (\tau_{0d}^2 - 1)^{\frac{1}{2}} = T_d(\tau_{0d})$, and so the singularity (in integrands (14) and (A2) near times $\tau = \tau_{0d}$) is indeed near that part of the real w-axis which is used for the integration. A further guide to properties of the w-plane Cagniard path is given by its closed form expression for points in the crack plane itself ($z = 0$, or $\theta = 90°$):

$$w = w_d(\tau)|_{z=0} = \begin{cases} i[-(F - \Sigma^2N^2\tau^2)^{\frac{1}{2}} + \Delta\tau]/F & \tau \leq F^{\frac{1}{2}}\Sigma^{-1}N^{-1} \\ [(\Sigma^2N^2\tau^2 - F)^{\frac{1}{2}} + i\Delta\tau]/F & \tau \geq F^{\frac{1}{2}}\Sigma^{-1}N^{-1} \end{cases} \tag{21}$$

This special case, also shown in Fig. 4, is an orthodox hyperbolic type of Cagniard path. In general, the remarks made above for $w_d(\tau)$ apply also to the shear wave terms and

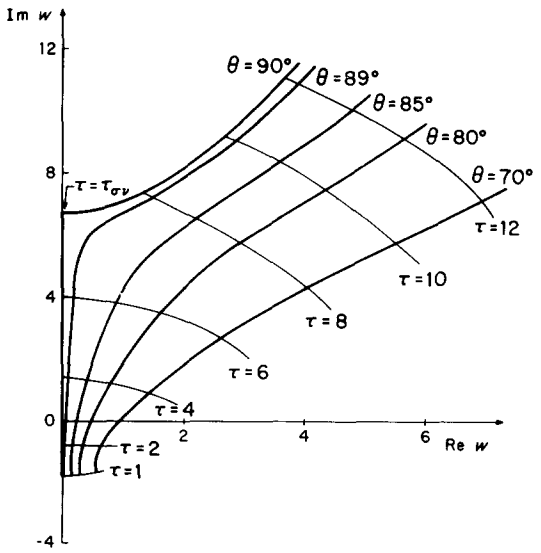

FIG. 4. Paths $w = w_d(\theta, \phi, \tau)$, calculated for $\phi = 45°$ at different θ and times $1 \leq \tau \leq 12$, using source parameters $c_s = c_d/\sqrt{3}$, $\sigma = c_d/2$, $\nu = c_d/10$. Note that for field points close to the crack itself ($\theta \to 90°$) these paths resemble an orthodox hyperbolic Cagniard path.

$w_s(\tau)$, and these two paths converge as $\tau \to \infty$. For points in the crack plane, the two paths are identical, $w_s(\tau)$ also being given by (21), and the q-plane Cagniard paths are simply $q_d(\tau) = i\tau = q_s(\tau)$ (independent of w).

With our knowledge of the location of the second order pole, in the integrand required for computation, and our knowledge of the times near which this singularity is close to the path of integration (the real w-axis, from $w = 0$ to $w = T_\alpha(\tau): \alpha = d$ or s), two techniques are suggested for avoiding problematical numerical effects. One can either move the path of integration (between its end points) into the complex w-plane, away from the singularity, or one can remove the singularity by subtracting out the first two terms in a Laurent series (in $w - w_\alpha(\tau)$), and integrating them separately. The first method does not lead to any obvious parameterization of the path of integration, so the second method has been developed, and has been found completely adequate. Relevant formulae are given in the Appendix.

In all the numerical problems examined to date, it has been found that the total solution appears completely smooth across times $\tau = \tau_{0d}$ and $\tau = \tau_{0s}$. This apparently is a consequence of the cancelling discontinuity in the integral of the second term in the Laurent series, as the pole migrates across the path of integration (see (A4)).

Singularities near the crack tip

The solution for $\partial^3\Phi/\partial t^3$, and for acceleration and stress rate components, contains a singularity for points in the crack plane. The singularity occurs at the time of the crack arrival, $t = t_{\sigma\nu}$ (say) where $t_{\sigma\nu} = (x^2/\sigma^2 + y^2/\nu^2)^{\frac{1}{2}}$, and may be seen in our solution as due to the singularity in $\partial w_\alpha/\partial t$ ($\alpha = d$ or s). Using dimensionless time, we have from (21) the

results $w_\alpha \sim i\Delta/(F^{\frac{1}{2}}\Sigma N)$ and

$$\frac{\partial w_\alpha}{\partial \tau} \sim i\Sigma N/[F(2\varepsilon)^{\frac{1}{2}}] \quad (\varepsilon > 0), \qquad \sim \Sigma N/[F(-2\varepsilon)^{\frac{1}{2}}] \quad (\varepsilon < 0) \tag{22}$$

as $\varepsilon \to 0$, where $\varepsilon = (t_{\sigma v} - t)/t_{\sigma v} = (\tau_{\sigma v} - \tau)/\tau_{\sigma v}$ with $\tau_{\sigma v} = F^{\frac{1}{2}}\Sigma^{-1}N^{-1}$.

That two different formulae are needed for the derivative in (22), as the limit is taken from above or below, is to be expected from a study of the curve in Fig. 4 for $\theta = 90°$, with its abrupt change in direction at $\tau = \tau_{\sigma v}$.

To describe the singularity in our solution, it is advisable to look at the time integral of the solutions we have previously described, since then the singularity is integrable. That is, we examine the singularity in $\partial^2\Phi/\partial t^2$ (and velocity and stress-components). It is then clear that the singular term (derived from (16)) is due to $L\partial w_\alpha/\partial\tau$, and it may easily be shown that

$$(2\varepsilon)^{\frac{1}{2}}\frac{\partial^2\Phi}{\partial t^2} \sim -2\pi\frac{\Sigma N C c_d}{FR}LH(t - t_{\sigma v}),$$

in which $L = L(q_d, w_d, \tau_{\sigma v})$ is evaluated with $q = i\tau_{\sigma v}$ and w_d given by (22) (the resulting L then being real). If these manipulations are carried through also for the shear stress components in the crack plane, in the case of relief of the zx component of stress ($b = 0$), it is found that

$$\tau_{zx}(2\varepsilon)^{\frac{1}{2}} \sim \frac{H(\varepsilon)4\mu c_s^2 a}{\Sigma^2 c_d^3 F B_s}[(B_d - B_s)B_s N^2\cos^2\phi + \tfrac{1}{4}(\Sigma^2 B_s^2 F - N^2\cos^2\phi)(c_d^2/c_s^2)]$$

$$\tau_{zy}(2\varepsilon)^{\frac{1}{2}} \sim \frac{H(\varepsilon)4\mu c_s^2 a\cos\phi\sin\phi}{c_d^3 F B_s}[B_s B_d - B_s^2 - \tfrac{1}{4}(c_d^2/c_s^2)] \tag{23}$$

as $\varepsilon \to 0$, where $B_\alpha \equiv [(\Sigma^4\sin^2\phi + N^4\cos^2\phi)(\Sigma^2 N^2 F) - (c_d^2/c_\alpha^2)]^{\frac{1}{2}} (\alpha = d, s)$.

The singularities for $\dot{u}_x$, $\dot{u}_y$ and τ_{zz} may be found directly from their known values everywhere in the crack plane (see (4) and (2)). The final result here is then for $\dot{u}_z$, given by

$$\dot{u}_z(2\varepsilon)^{\frac{1}{2}} \sim \frac{H(\varepsilon)2c_s^2 N a\cos\phi}{\Sigma c_d^2 F^{\frac{1}{2}} B_s}[\tfrac{1}{2}\tau_s^2 + B_s^2 - B_d B_s]. \tag{24}$$

Burridge and Willis [10] have also given formulae for the shear stress singularities around the rupture front of an elliptical shear crack. Unfortunately, their results differ from the above equation (23), the difference essentially being their neglect of a term in the definition of B_α. The neglected term contains the factor $\cos^2\phi\sin^2\phi$, and their results are in agreement with equation (23) just for the special directions $\phi = 0$, $\phi = 90°$. The singularities given above are in complete agreement with the numerical results obtained (at various intermediate values of ϕ) from computation of the complete solution described in the Appendix. As Burridge and Willis have pointed out, the τ_{zx} singularity vanishes at $\phi = 0$ when σ is the Rayleigh wave speed c_R (say), and vanishes at $\phi = 90°$ when v is the shear wave speed c_s. These special directions correspond to local states of plane strain and anti-plane strain (respectively), and such states may be analyzed as two-dimension problems of crack propagation. If brittle fracture is an adequate model of material failure, then the ellipse given by $\sigma = c_R$, $v = c_s$ is suggested as the parameterization for a steadily

growing crack: it would of course be desirable to drop the constraints of holding σ and v constant, but the resulting elasticity problem is as yet unsolved.

5. SOME NUMERICAL EXAMPLES, FOR RELIEF OF THE ZX-COMPONENT OF STRESS

The Appendix formulae have been programmed in FORTRAN, using real arithmetic only, for evaluation on an IBM 1130 computer. Input parameters are the velocity ratios Σ, N and c_s/c_d, and dimensionless space–time coordinates (θ, ϕ, τ), and output is the dimensionless accelerations $\ddot{u}_i \times (\pi c_d^3 R)/(8c_s^2 \sigma v a)$ and dimensionless stress rates $\dot{t}_{iz} \times (\pi c_d^4 R)/(16\mu c_s^2 \sigma v a)$ $(i = x, y \text{ or } z)$. If the residue terms (16) or (A3) are required, values of $w_\alpha(\tau)$ $(\alpha = d \text{ or } s)$ are obtained for given time τ by the iteration

$$w_{n+1} = w_n + (\tau - Z(w_n))/(\partial Z(w_n)/\partial w), \quad n = 1, 2, \ldots$$

where

$$Z = [-iq \sin \theta + (q^2 + w^2 + c_d^2/c_\alpha^2)^{\frac{1}{2}} \cos \theta]|_{q = q_{\sigma v}(w)}.$$

The starting value w_1 is obtained either from the asymptotic approximation of (15c), or from a value of w_α previously found on the Cagniard path for nearby τ. The iteration has been found to converge rapidly, in all cases tried.

Numerical checks of the program have been made to ensure that: (a) the dilatational component of acceleration is irrotational; (b) the shear wave component is solenoidal; (c) $\rho \ddot{u}_z = \dot{t}_{zx,x} + \dot{t}_{zy,y} + \dot{t}_{zz,z}$ (i.e. the z component of the equation of motion is satisfied); (d) boundary conditions (2) and (4) are satisfied; (e) τ_{zx} is constant over the crack surface, for given $(\Sigma, N, c_s/c_d)$; and (f) that the computed values agree with the wavefront formulae and crack tip singularities in equations (18), (19), (23) and (24).

Since some of the most interesting features of crack propagation are contained in the vicinity of the crack tip, computations are presented below† for the case $\theta = 85°$. Two different azimuths are used, $\phi = 1°$ and $\phi = 89°$ (corresponding respectively to states essentially of plane strain and anti-plane strain), and times include those at which the crack tip passes nearby. Rupture speeds are taken as $(\sigma, v) = (\kappa c_R, \kappa c_s)$, where κ takes on four different values 0·5, 0·7, 0·9 and 1·0. This last value of κ is that suggested by results of the previous section, giving rupture speeds which reduce the stress concentrations around the crack tip. Lamé parameters λ and μ are taken as equal, so $c_d/c_s = \sqrt{3}$.

Example I: $\phi = 1°$

In Figs. 5, 6, 7 and 8 are shown the x and z components of acceleration, and zx and zz components of stress rate. Principal features of these computations are: (a) the large radiation at times when the crack tip is nearby (i.e. large relative to the wavefront values at times $\tau = 1$, $\tau = \sqrt{3}$). In fact, the four curves in each of these four figures all have a zero-crossing very close to the time of nearest approach of the crack tip, indicating that velocity and stress components all have maximum magnitudes near this time; (b) the increase in maximum amplitudes as the rupture velocities increase. This effect is accentuated for the dimensional variables, which are proportional to κ^2 times the values plotted;

† The computations described in this section required about 5 h of time on an IBM 1130, or 80 sec on a Univac 1108.

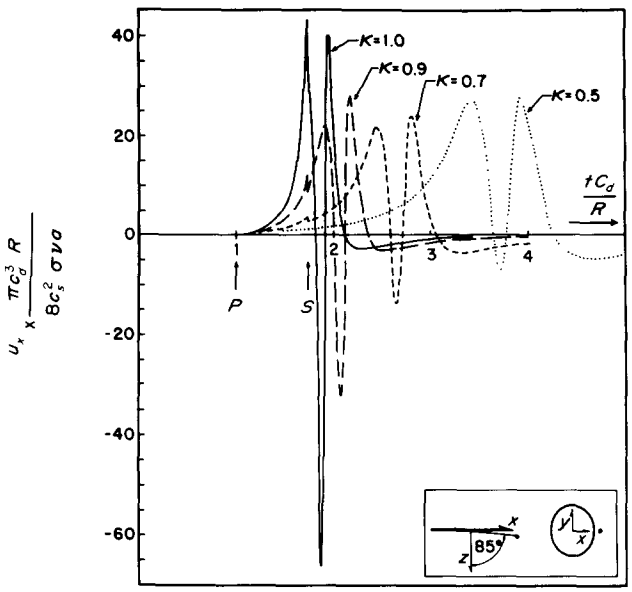

FIG. 5. The x-component of acceleration, due to relief of the zx component of stress, at points along $\theta = 85°$, $\phi = 1°$ (see insert). Computation is done for four different rates of crack growth: $(\sigma, v) = (\kappa c_R, \kappa c_s)$, with $\kappa = 0{\cdot}5$, $0{\cdot}7$, $0{\cdot}9$, $1{\cdot}0$, and corresponding times at which the crack tip passes nearby are $tc_d/R = 3{\cdot}76$, $2{\cdot}69$, $2{\cdot}09$, $1{\cdot}87$. Arrows at P and S mark the arrival times of P- and S-waves from the original point of rupture.

(c) the wavefront discontinuity for shear waves becomes significant as $\kappa \to 1{\cdot}0$. This is to be expected physically, since then in the direction $(\theta, \phi) = (85°, 1°)$ the shear wavefront is followed closely by the radiation from the crack tip; and (d) the curves for $\ddot{u}_x$ tend to zero, as τ increases, but more slowly than do the curves for $\dot{\tau}_{zx}$ and $\dot{\tau}_{zz}$. This is to be expected from the known formulae for these three variables on the crack surface itself. Figure 6

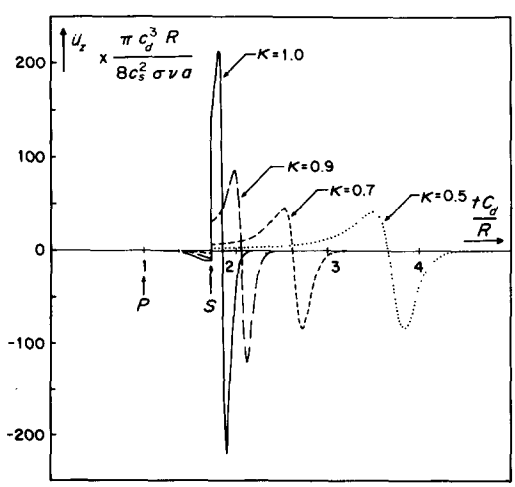

FIG. 6. As for Fig. 5, but showing the z component of acceleration.

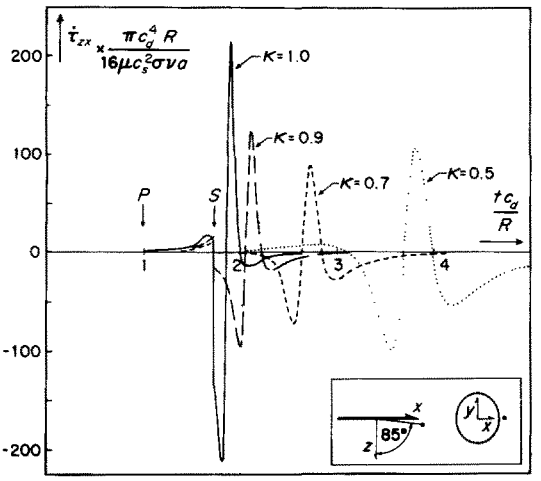

FIG. 7. As for Fig. 5, but showing the zx component of stress rate.

shows also that $\ddot{u}_z$ tends rapidly to zero as τ increases, and further work has shown that it also (with $\dot{\tau}_{zx}$ and $\dot{\tau}_{zz}$) vanishes on the crack surface.

Example II: $\phi = 89°$

In Figs. 9 and 10 are shown the x component of acceleration, and zx component of stress rate. Principal features here are the off-scale values for $\kappa = 1{\cdot}0$, near the shear wave arrival time. For the direction $(\theta, \phi) = (85°, 89°)$, and $v = c_s$, the crack tip radiation essentially is riding on the shear wavefront. And the wavefront discontinuity (see equation (19)) is proportional to $(1 - D(c_d/c_s)^2 \sin^2\theta)^{-2}$, which here (for $\kappa = 1$, $\phi \sim 90°$) is approximately $1/\cos^4\theta$. It is simple to show that $\ddot{u}_y$, $\ddot{u}_z$, $\dot{\tau}_{yz}$, $\dot{\tau}_{zz}$ are proportional to $\cos\phi$, if ϕ is near 90°, and so are very small. Motion near this azimuth thus lacks a longitudinal component.

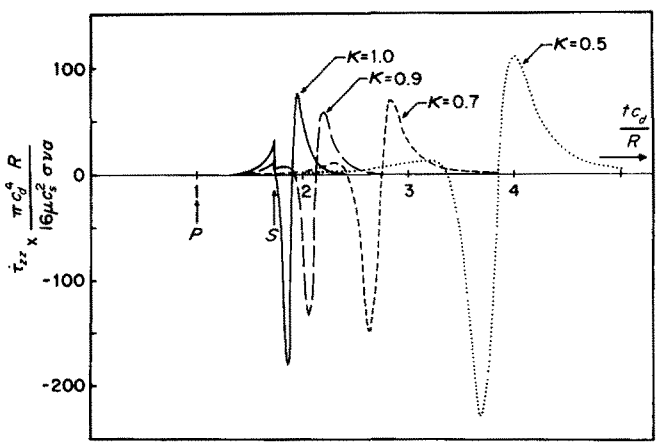

FIG. 8. As for Fig. 5, but showing the zz component of stress rate.

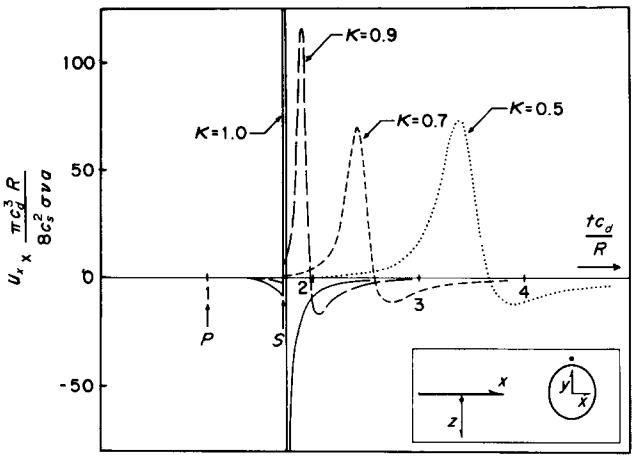

FIG. 9. The x-component of acceleration, due to relief of the zx component of stress, at points along $\theta = 85°$, $\phi = 89°$ (see insert). Computation is done for crack growth $(\sigma, v) = (\kappa c_R, \kappa c_s)$ with $\kappa = 0{\cdot}5$, $0{\cdot}7, 0{\cdot}9, 1{\cdot}0$, and corresponding times at which the crack tip passes nearby are $tc_d/R = 3{\cdot}45, 2{\cdot}46, 1{\cdot}92, 1{\cdot}72$.

Finally, it should be pointed out that interpretation of Figs. 5–10, in application to a particular problem, requires knowledge of the dimensioning factors which have been included in the plotted values. In particular, the value of a (the initial particle velocity at the point of crack nucleation) is often needed. For the faulting which occurs during an earthquake, it has been suggested by Brune [13] that near-source particle velocities have an upper limit of about 100 cm/sec (3 ft/sec).

6. CONCLUSIONS

The exact solution, for the dynamic field of a steadily growing elliptical shear crack, may be obtained in a form sufficiently simple for rapid numerical calculation. The technique involves first the setting up of the correct boundary value problem, in terms of the displacement continuity across the crack, and second the repeated use of Cagniard–de Hoop

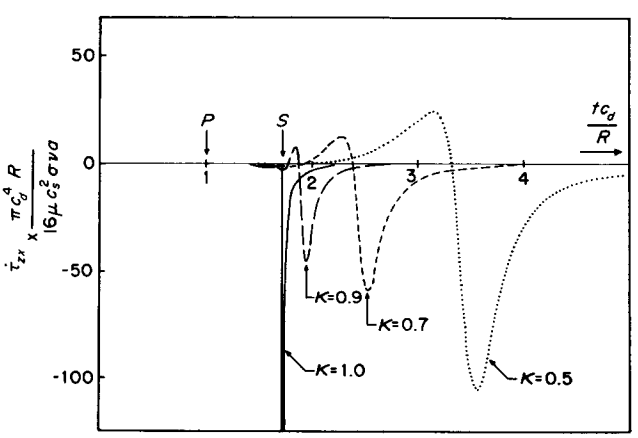

FIG. 10. As for Fig. 9, but showing the zx component of stress rate.

procedures. The solution is found in terms of single integrals (a common feature of transient elastic solutions in three dimensions), plus algebraic terms which require the numerical evaluation of a fourth-order Cagniard path.

The problem solved here has no inherent scaling, so the solution is of relevance to the study of rupture phenomena ranging from micro-fracturing to large earthquakes.

Acknowledgements—The author thanks Drs. L. A. Alsop, D. C. Gakenheimer and C. H. Scholz for their critical reading of the manuscript.

This research was supported by the Advanced Research Projects Agency of the Department of Defense, and was monitored by the Air Force Cambridge Research Laboratories under Contract No. F19628-71-C-0245.

REFERENCES

[1] E. H. YOFFE, The moving Griffith crack. *Phil. Mag.* **42**, 739 (1951).
[2] K. B. BRODBERG, The propagation of a brittle crack. *Arkiv för Fysik* **18**, 159 (1960).
[3] B. R. BAKER, Dynamic stresses created by a moving crack. *J. appl. Mech.* **29**; *Trans. ASME* **84**, 449 (1962).
[4] B. V. KOSTROV, The axisymmetric problem of propagation of a tension crack. *J. appl. Math. Mech.* **28**, 793 (1964).
[5] J. W. CRAGGS, The growth of a disk-shaped crack. *Int. J. Eng. Sci.* **4**, 113 (1966).
[6] B. V. KOSTROV, The theory of the focus for tectonic earthquakes, *Izvestiya, Solid Earth Physics* 258 (1970).
[7] B. V. KOSTROV, Selfsimilar problems of propagation of shear cracks. *J. appl. Math. Mech.* **28**, 1077 (1964).
[8] B. V. KOSTROV, Unsteady propagation of longitudinal shear cracks, *J. appl. Math. Mech.* **30**, 1241 (1966).
[9] R. BURRIDGE, The numerical solution of certain integral equations with non-integrable kernels arising in the theory of crack propagation and elastic wave diffraction. *Phil. Trans. R. Soc. (London)* **A 265**, 353 (1969).
[10] R. BURRIDGE and J. R. WILLIS, The self-similar problem of the expanding elliptical crack in an anisotropic solid. *Proc. Cambridge Phil. Soc.* **66**, 443 (1969).
[11] D. C. GAKENHEIMER and J. MIKLOWITZ, Transient excitation of an elastic half space by a point load traveling on the surface. *J. appl. Mech.* **36**; *Trans. ASME* **91 E**, 505 (1969).
[12] D. C. GAKENHEIMER, Response of an elastic half space to expanding surface loads. *J. appl. Mech.* **38**; *Trans. ASME* **93 E**, 99 (1971).
[13] J. N. BRUNE, Tectonic stress and the spectra of seismic shear waves from earthquakes. *J. Geophys. Research* **75**, 4997 (1970).

APPENDIX

Solution formulae, for relief of the zx component of stress.

For components of acceleration and stress-rate, the solution takes the form

$$\ddot{u}_j = \frac{8c_s^2\sigma va}{\pi c_d^3 R}\{I_d + I_s + R_d + R_s\}$$

$$\dot{\tau}_{jz} = \frac{16\mu c_s^2\sigma va}{\pi c_d^4 R}\{I_d + I_s + R_d + R_s\} \qquad j = x, y \text{ or } z \tag{A1}$$

in which† the integral terms (I_α: $\alpha = d$ or s) and residue terms (R_α) are

$$I_\alpha = H(\tau - \tau_\alpha)\int_0^{T_\alpha} \mathrm{Re}\left\{\frac{(E^2+O^2)M_\alpha - 2EON_\alpha}{(E^2-O^2)^2}\frac{\partial q_\alpha}{\partial \tau}\right\} \mathrm{d}w \tag{A2}$$

$$R_\alpha = 2\pi H(G)H(\tau - \tau_{0\alpha})\,\mathrm{Re}\, i\{-[U_\alpha + iV_\alpha D/a_1]a_2/(8a_1^2) + a_{11}a_2 W_\alpha + a_{12}V_\alpha\} \tag{A3}$$

† A dot (˙) denotes the derivative $\partial/\partial t$ (with respect to dimensioned time).

with M_α, N_α, U_α, V_α, W_α ($\alpha = d, s$) given in Tables 2 and 3 (as a function of the dimensionless time $\tau = tc_d/R$), and $\tau_\alpha = c_d/c_\alpha$, $T_\alpha = (\tau^2 - \tau_\alpha^2)^{\frac{1}{2}}$, E and O as in equation (9) with $q = q_\alpha$ given by (11) or (17), G as in (12) and $\tau_{0\alpha} = (w_{0\alpha}^2 \Sigma^2 N^2 + D)^{\frac{1}{2}} \operatorname{cosec} \theta / D$ where

$$w_{0\alpha}^2 = D \cos^2 \theta (1 - D\tau_\alpha^2 \sin^2 \theta)/G.$$

TABLE 2. A LIST OF THE FUNCTIONS NEEDED IN EQUATION (A2), TO OBTAIN THE INTEGRAL CONTRIBUTION TO SOLUTIONS FOR ACCELERATION AND STRESS RATE: q IS TAKEN AS THE CAGNIARD PATH VALUE $q_d(t)$ FOR THE DILATATIONAL TERMS M_d, N_d, AND AS $q_s(t)$ FOR SHEAR TERMS M_s, N_s

Solution	M_d	N_d
$\ddot{u}_x$	$-q^2 \cos^2 \phi - w^2 \sin^2 \phi$	$2qw \cos \phi \sin \phi$
$\ddot{u}_y$	$(-q^2 + w^2) \cos \phi \sin \phi$	$-qw(\cos^2 \phi - \sin^2 \phi)$
$\ddot{u}_z$	$-iqm_d \cos \phi$	$iwm_d \sin \phi$
$\dot{\tau}_{zx}$	$m_d(q^2 \cos^2 \phi + w^2 \sin^2 \phi)$	$-2qwm_d \cos \phi \sin \phi$
$\dot{\tau}_{zy}$	$m_d(q^2 - w^2) \cos \phi \sin \phi$	$qwm_d(\cos^2 \phi - \sin^2 \phi)$
$\dot{\tau}_{zz}$	$i(q^2 + w^2 + \frac{1}{2}\tau_s^2)q \cos \phi$	$-i(q^2 + w^2 + \frac{1}{2}\tau_s^2)w \sin \phi$
f	M_s	N_s
$\ddot{u}_x$	$q^2 \cos^2 \phi + w^2 \sin^2 \phi + \frac{1}{2}\tau_s^2$	$-2qw \cos \phi \sin \phi$
$\ddot{u}_y$	$(q^2 - w^2) \cos \phi \sin \phi$	$qw(\cos^2 \phi - \sin^2 \phi)$
$\ddot{u}_z$	$iq(m_s - \frac{1}{2}\tau_s^2/m_s) \cos \phi$	$-iw(m_s - \frac{1}{2}\tau_s^2/m_s) \sin \phi$
$\dot{\tau}_{zx}$	$(-q^2 \cos^2 \phi - w^2 \sin^2 \phi)(m_s - \frac{1}{4}\tau_s^2/m_s) - \frac{1}{4}\tau_s^2 m_s$	$2qw(m_s - \frac{1}{4}\tau_s^2/m_s) \cos \phi \sin \phi$
$\dot{\tau}_{zy}$	$(-q^2 + w^2)(m_s - \frac{1}{4}\tau_s^2/m_s) \cos \phi \sin \phi$	$-qw(m_s - \frac{1}{4}\tau_s^2/m_s)(\cos^2 \phi - \sin^2 \phi)$
$\dot{\tau}_{zz}$	$-i(q^2 + w^2 + \frac{1}{2}\tau_s^2)q \cos \phi$	$i(q^2 + w^2 + \frac{1}{2}\tau_s^2)w \sin \phi$

TABLE 3. A LIST OF THE FUNCTIONS NEEDED IN EQUATION (A3), TO OBTAIN THE RESIDUE CONTRIBUTION TO SOLUTIONS FOR ACCLERATION AND STRESS RATE: w IS TAKEN AS THE CAGNIARD PATH VALUE $w_\alpha(t)$ ($\alpha = d$ OR s), AND q AS THE SINGULAR VALUE $q_{\sigma v}(w_\alpha)$

Solution	U_d	V_d	W_d
$\ddot{u}_x$	$-2a_4 \cos \phi$	$-a_4^2$	$-2a_4a_8$
$\ddot{u}_y$	$-a_6$	$-a_5$	$-a_9$
$\ddot{u}_z$	$-i(m_d \cos \phi + qa_4/m_d)$	$-ia_4m_d$	$-i(a_8m_d + a_4a_{10}/m_d)$
$\dot{\tau}_{zx}$	$2a_4m_d \cos \phi + qa_4^2/m_d$	$a_4^2m_d$	$2a_4a_8m_d + a_4^2a_{10}/m_d$
$\dot{\tau}_{zy}$	$a_6m_d + qa_5/m_d$	a_5m_d	$a_9m_d + a_5a_{10}/m_d$
$\dot{\tau}_{zz}$	$i(a_{13} \cos \phi + 2qa_4)$	ia_4a_{13}	$i(a_8a_{13} + 2a_4a_{10})$
f	U_s	V_s	W_s
$\ddot{u}_x$	$2a_4 \cos \phi$	$a_4^2 + \frac{1}{2}\tau_s^2$	$2a_4a_8$
$\ddot{u}_y$	a_6	a_5	a_9
$\ddot{u}_z$	$i(a_{71} \cos \phi + a_4a_{73})$	ia_4a_{71}	$i(a_8a_{71} + a_4a_{10}a_{73}/q)$
$\dot{\tau}_{zx}$	$-2a_4a_{72} \cos \phi - a_4^2a_{74} - \frac{1}{4}\tau_s^2 q/a_7$	$-a_4^2a_{72} - \frac{1}{4}\tau_s^2a_7$	$-2a_4a_8a_{72} - (a_4^2a_{74}/q + \frac{1}{4}\tau_s^2/a_7)a_{10}$
$\dot{\tau}_{zy}$	$-a_6a_{72} - a_5a_{74}$	$-a_5a_{72}$	$-a_9a_{72} - a_5a_{10}a_{74}/q$
$\dot{\tau}_{zz}$	$-i(a_{13} \cos \phi + 2qa_4)$	$-ia_4a_{13}$	$-i(a_8a_{13} + 2a_4a_{10})$

Cagniard paths $w = w_\alpha(\tau)(\alpha = d, s)$ are defined in the first quadrant of the complex w-plane by finding solutions to

$$\tau = [-iq\sin\theta + (q^2 + w^2 + \tau_\alpha^2)^{\frac{1}{2}}\cos\theta]|_{q=q_{\sigma v}(w)} \quad \text{where } q_{\sigma v} = [w\Delta + i(w^2\Sigma^2N^2 + D)^{\frac{1}{2}}]D.$$

With $w = w_\alpha(\tau)$ and $q = q_{\sigma v}(w_\alpha(\tau))$, the following time-dependent (and wave-type dependent) functions, needed in Tables 2 and 3, are finally defined:

$$a_1 = (w^2\Sigma^2N^2 + D)^{\frac{1}{2}} \qquad a_2 = \partial w_\alpha/\partial\tau \qquad a_3 = \mathrm{d}q_{\sigma v}/\mathrm{d}w$$

$a_4 = q\cos\phi \mp w\sin\phi$, where the upper or lower sign is taken, according as

$$(\sigma^2 - v^2)\sin 2\phi \gtrless 0, \qquad a_5 = (q^2 - w^2)\cos\phi\sin\phi \pm qw(\cos^2\phi - \sin^2\phi)$$

$$a_6 = 2q\cos\phi\sin\phi \pm w(\cos^2\phi - \sin^2\phi) \qquad a_7 = m_s = (q^2 + w^2 + \tau_s^2)^{\frac{1}{2}}$$

$$a_{71} = m_2 - \tfrac{1}{2}\tau_s^2/m_s \qquad a_{72} = m_s - \tfrac{1}{4}\tau_s^2/m_s \qquad a_{73} = q/m_s + \tfrac{1}{2}q\tau_s^2/m_s^3$$

$$a_{74} = q/m_s + \tfrac{1}{4}q\tau_s^2/m_s^3 \qquad a_8 = a_3\cos\phi \mp \sin\phi$$

$$a_9 = 2(qa_3 - w)\cos\phi\sin\phi \pm (wa_3 + q)(\cos^2\phi - \sin^2\phi) \qquad a_{10} = qa_3 + w$$

$$a_{11} = \{8a_1^2[a_3 + w\cos\theta/(q\cos\theta - im_\alpha\sin\theta)]\}^{-1}$$

$$a_{12} = da_{11}/\mathrm{d}\tau \qquad a_{13} = q^2 + w^2 + \tfrac{1}{2}\tau_s^2.$$

The factor $\{\ \}$, in solution formulae (A1), is a dimensionless quantity dependent only on (θ, ϕ, τ), but not on R. The radiated pulse shapes are thus the same, for all points along a given straight line through the point of initial rupture. This self-similar property is noted in [7], [10] and [12], and is the basis for applying numerical results of Figs. 5–10 to problems of (small-scale) material failure, and to the study of earthquakes.

Finally, in order to carry out the numerical integration of (A2), it is often convenient to subtract out from the integrand the singularity arising from a double zero in $(E^2 - O^2)^2$ at the value $w = w_\alpha(\tau)$. (See text, discussion of (20).) To this end, it may be noted that

$$(E^2 - O^2)^2 = (w - w_\alpha)^2(8q_\alpha w_\alpha\Delta)^2a_{14}^2[1 + (w - w_\alpha)(a_{15} + a_{16})] + 0[(w - w_\alpha)^4]$$

as $w \to w_\alpha(\tau)$, where

$$a_{14} = wF - q\Delta + ia_1\partial q/\partial w$$

$$a_{15} = Fa_{17} - (\partial q/\partial w)(\Delta + q\Sigma^2N^2a_{17})a_{17} + [ia_1(\partial^2 q/\partial w^2) - (\partial q/\partial w)^2\Sigma^2N^2a_{17}^2]/a_{14}$$

$$a_{16} = 1/w + F/(q\Delta) + (\partial q/\partial w)[1/q + D/(w\Delta)] \qquad a_{17} = 1/(wF - q\Delta)$$

in which $q = q_\alpha(w_\alpha(\tau), \tau)$, $w = w_\alpha(\tau)$.

The integrand for I_α in (A2) thus has singularities obtainable from a Laurent series as

$$S_\alpha = \mathrm{Re}\{X_\alpha/(w - w_\alpha)^2 + Y_\alpha/(w - w_\alpha)\}$$

in which

$$X_\alpha = a_{18}V_\alpha/(8a_{14}^2), \qquad Y_\alpha = [(a_{19} - a_{15}a_{18})V_\alpha + a_{18}W_\alpha']/(8a_{14}^2),$$

where

$$a_{18} = \tau(\tau^2 - w_\alpha^2 - \tau_\alpha^2)^{-\frac{1}{2}} \cos\theta + i \sin\theta, \qquad a_{19} = w_\alpha \tau(\tau^2 - w_\alpha^2 - \tau_\alpha^2)^{-\frac{1}{2}} \cos\theta,$$

and W'_α is defined by the W_α of Table 3, but with a_3 $(= \partial q_{\sigma v}/\partial w)$ replaced by $a'_3 = \partial q_\alpha/\partial w$.

If the singularity S_α is subtracted from the integrand for I_α, there results a smooth integrand which is amenable to numerical calculation† at all times τ. An extra term, the integral of S_α, must then be added to obtain I_α itself. This extra term is simply

$$\int_0^{T_\alpha} S_\alpha \, dw = \mathrm{Re}\{X_\alpha T_\alpha/[w_\alpha(w_\alpha - T_\alpha)] + Y_\alpha[\log|1 - T_\alpha/w_\alpha| + i \arg(1 - T_\alpha/w_\alpha)]\} \qquad \text{(A4)}$$

which is seen to be discontinuous as time increases through $\tau = \tau_{0\alpha}$, since w_α crosses the real w-axis (at $w = w_{0\alpha}$), and the angle $\arg(1 - T_\alpha/w_\alpha)$ jumps up through 2π.

(*Received* 15 *September* 1972; *revised* 15 *November* 1972)

Абстракт—Исследуется излучение для трехмерной задачи хрупкого разрушения. Предполагается что трещина служит центром для развития процесса, в некоторой точке бесконечной, предварительно напряженной, упругой среде и, далее, трещина впоследствии постоянно увеличивается с дозвуковыми скоростьями разрушения, утверждая форму элипса. Напряжения сдвига уменьшаются вследствие трещины. Выводятся строгие решения для ускорения и скорости напряжений (для каждой точки среды), в виде простых интегралов и алгебраических выражений. Дается аналитическая оценка решений для фронтов волн и особых точек, и численная, для разных точек среды, для разного роста скоростей трещины.

† These integrands are typical of Cagniard solutions in that they exhibit a singularity at the upper limit, due to the $\partial q_\alpha/\partial\tau$ factor. This singularity is removed by the substitution $w = T_\alpha \sin\chi$, and integrating the range $0 \le \chi \le \pi/2$.